

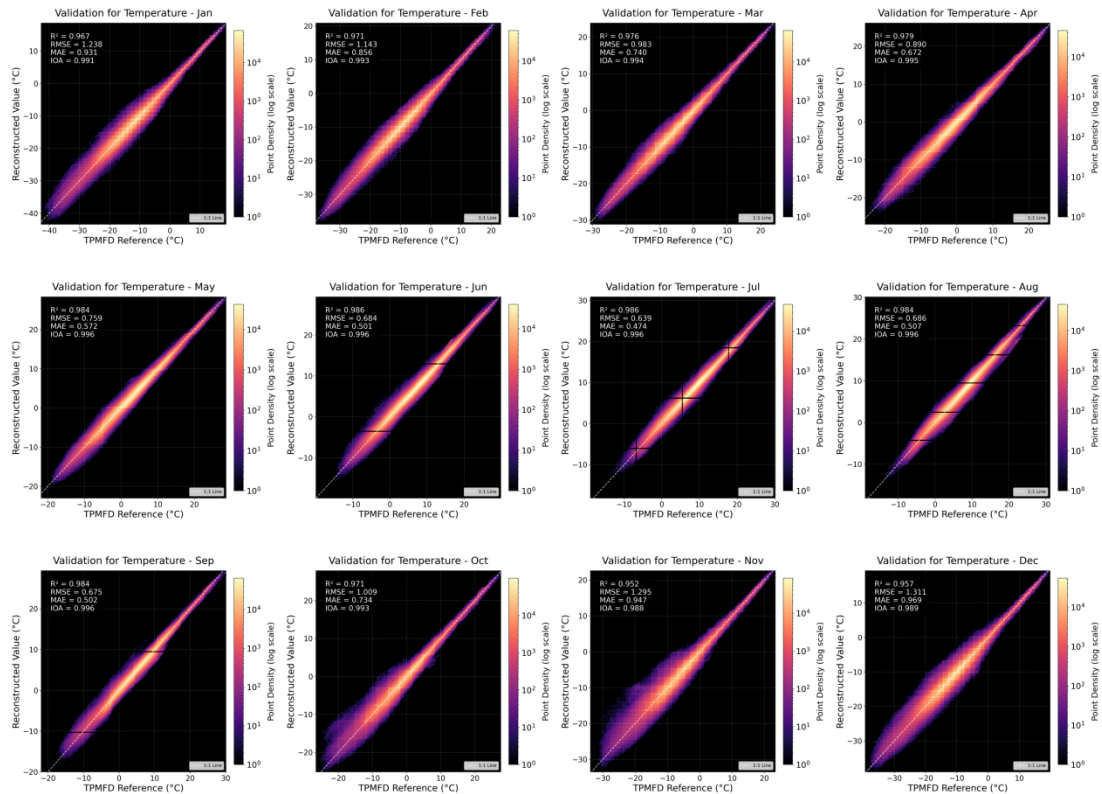
**TPHH: A long-term (1901–2023) high-resolution (1/30°) near-surface
humidity dataset for the Tibetan Plateau generated via spatial
downscaling based on hybrid-structure deep learning**

Contents of this file

Figures S1 to S13

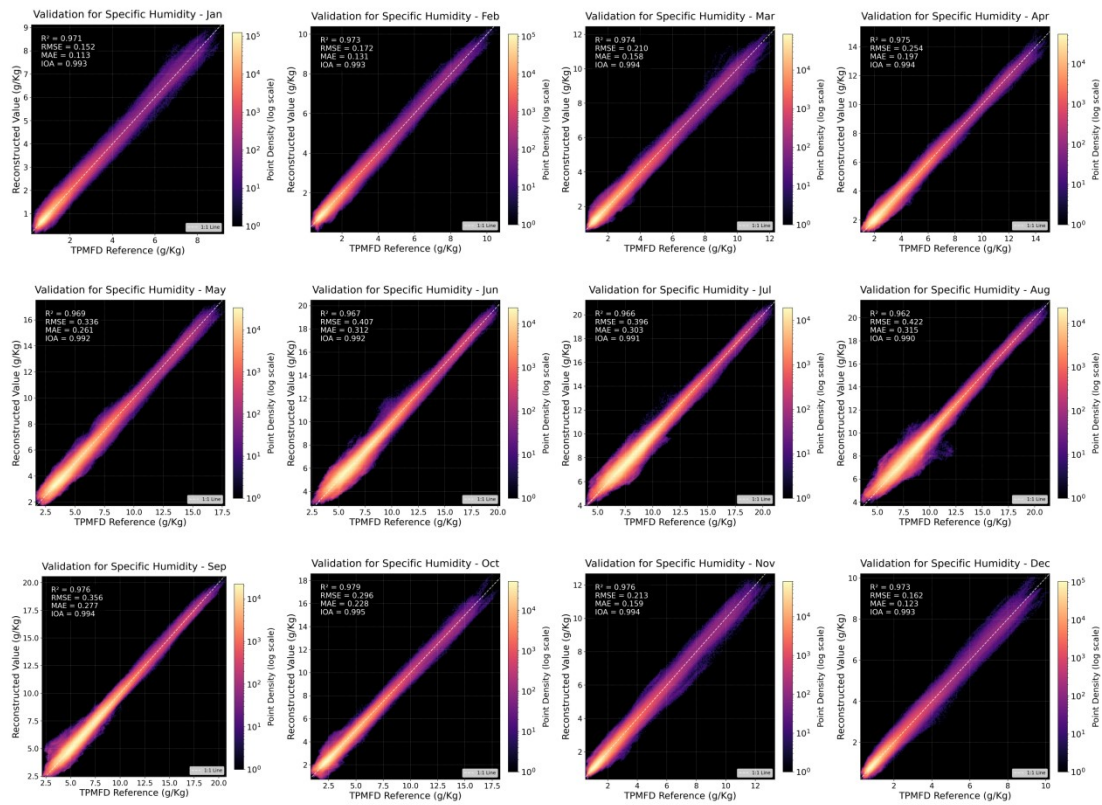
Introduction

In these supplementary materials, we gathered monthly density scatter plots for 2 m temperature (**Figure S1**), 2 m specific humidity (**Figure S2**), and surface pressure (**Figure S3**), monthly interannual curves for those three variables (**Figure S4-6**), compares the proposed TPHH product against two representative datasets (**Figure S7**), distribution of the 41 tree-ring proxy groups as well as each sample over the Tibetan Plateau (**Figure S8**), and tree-ring proxy fitting results for all 41 sample groups (**Figure S9-13**).



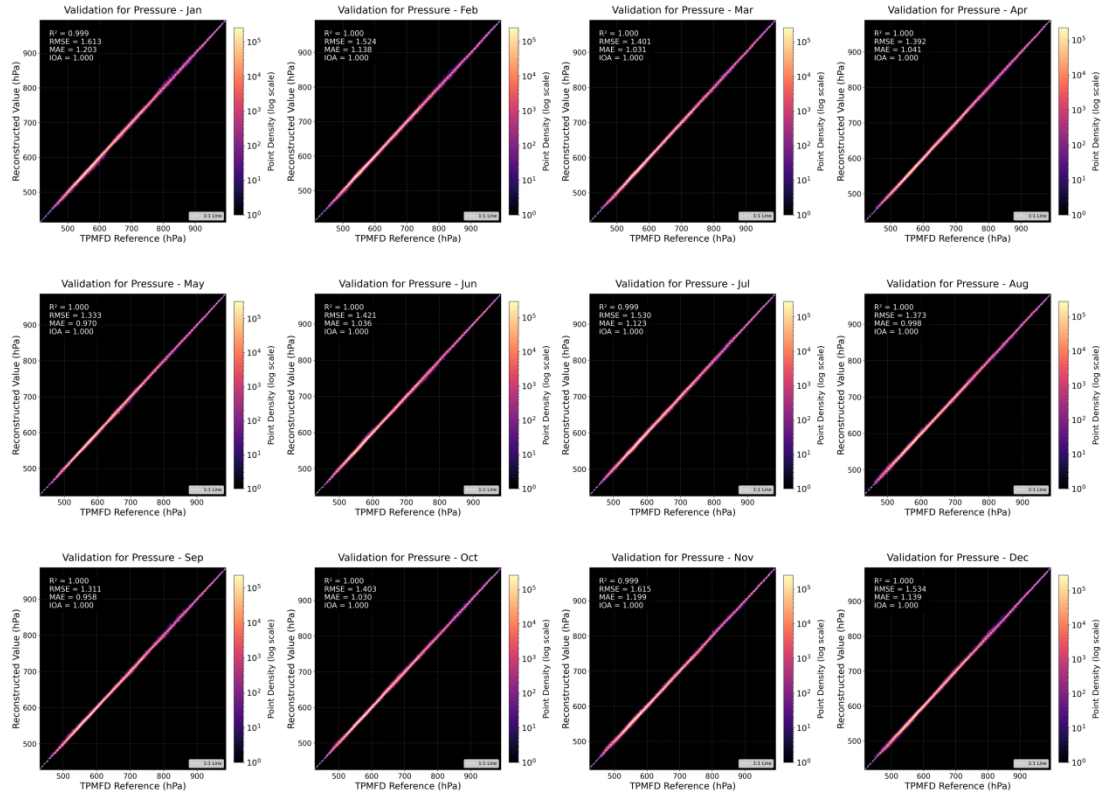
14

15 **Figure S1.** Monthly validation of the downscaled 2 m temperature (Temp). Density scatter plots
 16 comparing the THPP reconstructed high-resolution temperature values against the TPMFD reference
 17 data across all 12 months. The dashed line represents the 1:1 reference line of perfect agreement. Color
 18 gradients indicate point density (logarithmic scale), with warmer colors representing higher
 19 concentrations of data points. Statistical metrics including the coefficient of determination (R^2), Root
 20 Mean Square Error (RMSE), Mean Absolute Error (MAE), and Index of Agreement (IOA) for each
 21 specific month are inset in the upper-left corner of the respective panels.



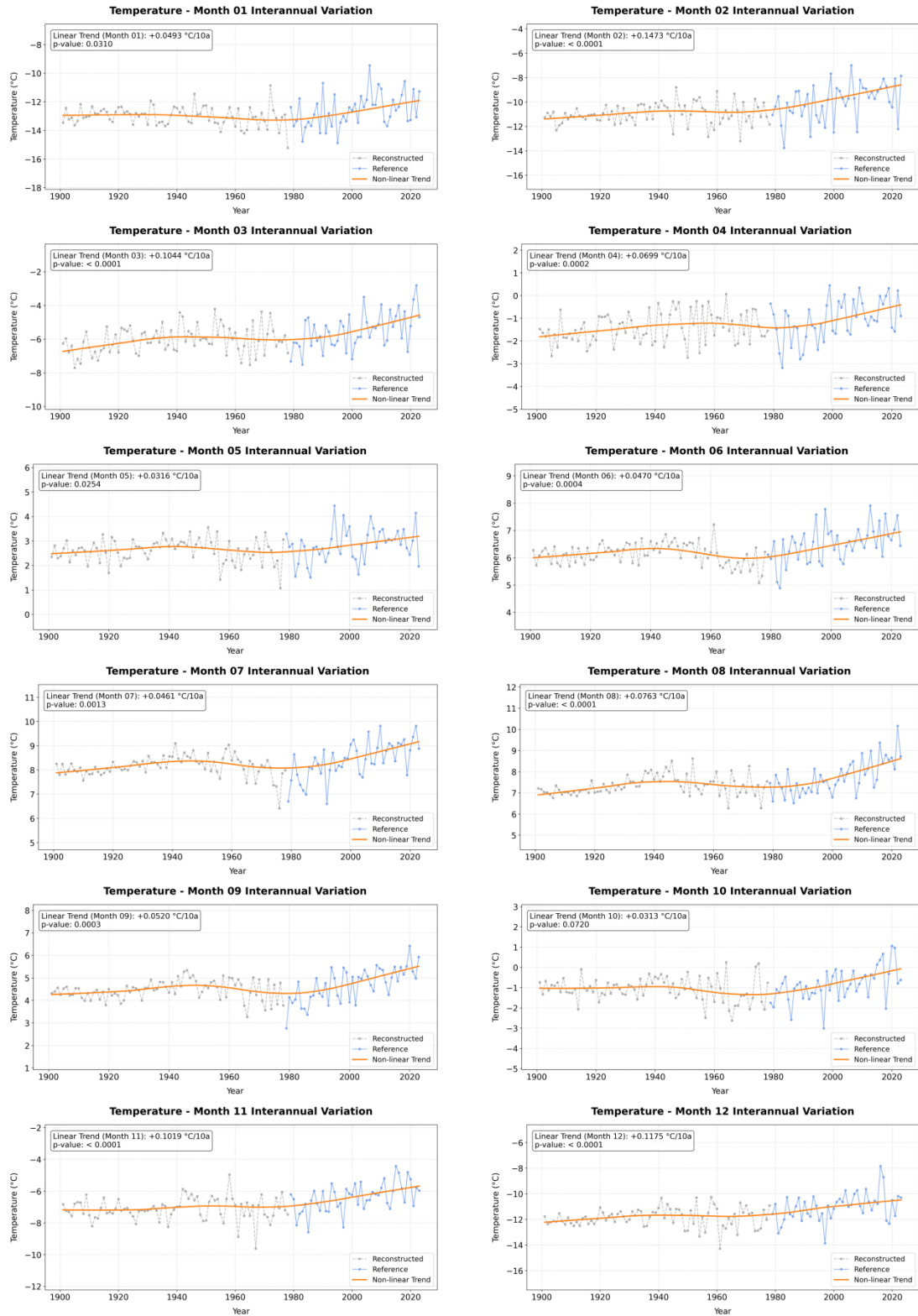
22

23 **Figure S2.** Monthly validation of the downscaled specific humidity (Shum). Density scatter plots
 24 comparing the THPP reconstructed high-resolution specific humidity values against the TPMFD
 25 reference data across all 12 months. The dashed line represents the 1:1 perfect agreement line. Point
 26 density is mapped to the color gradient on a logarithmic scale. Inset evaluation metrics (R^2 , RMSE, MAE,
 27 and IOA) quantify the model's monthly performance.



28

29 **Figure S3.** Monthly validation of the downscaled surface pressure (Pres). Density scatter plots showing
 30 the correlation between the THPP reconstructed high-resolution surface pressure and the corresponding
 31 TPMFD reference data for each month. The 1:1 reference line is indicated by the dashed line. The color
 32 bar reflects the point density distribution (logarithmic scale). Quantitative metrics (R^2 , RMSE, MAE,
 33 and IOA) derived from the masked evaluation over the Tibetan Plateau are provided in the upper-left
 34 corners.

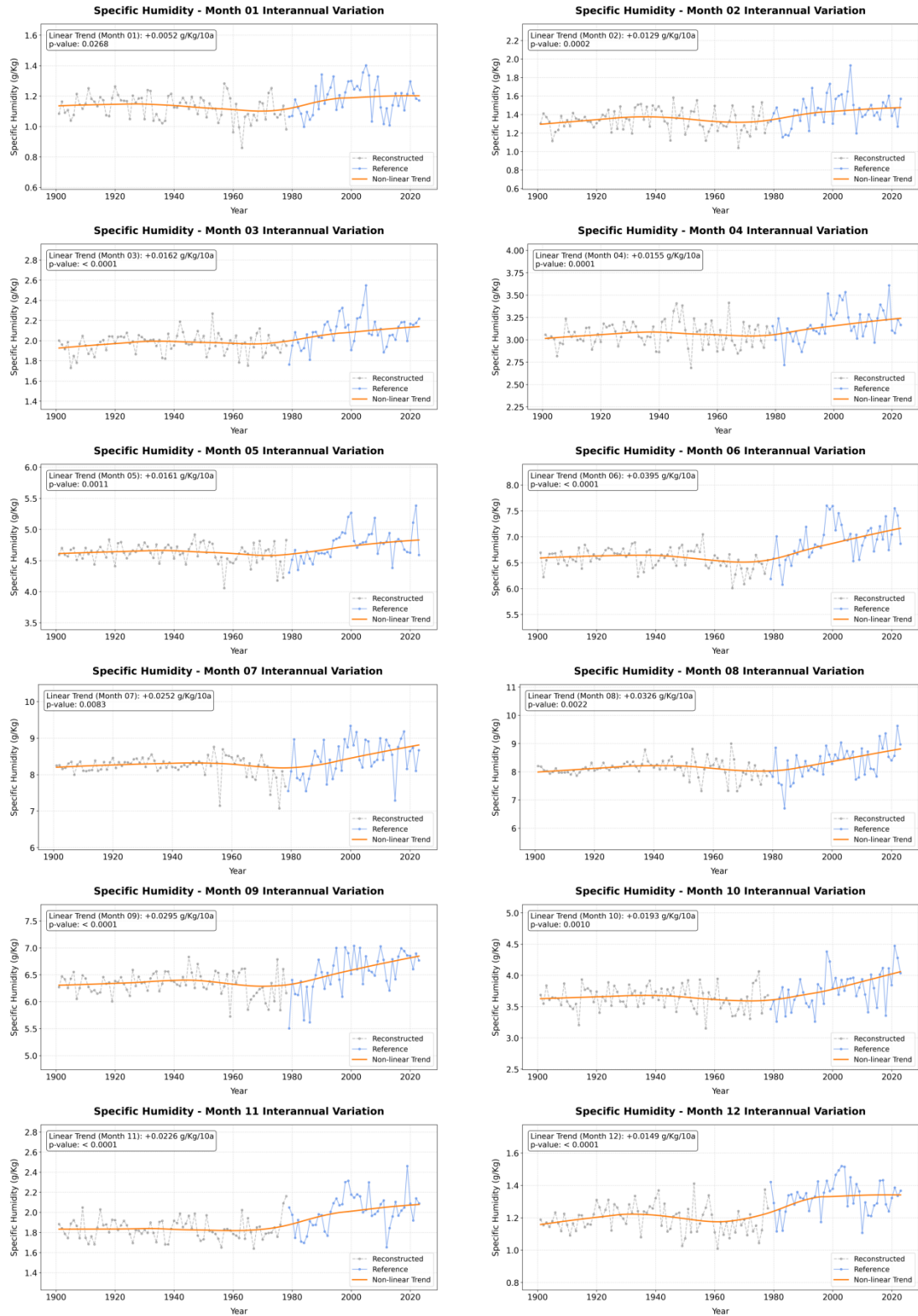


35

36 **Figure S4.** Monthly interannual variations of 2 m temperature over the Tibetan Plateau (1901–2023).

37 Grey dashed and solid blue lines denote the reconstructed (1901–1978) and reference (1979–2023) data,

38 respectively. The orange curve indicates the trend.

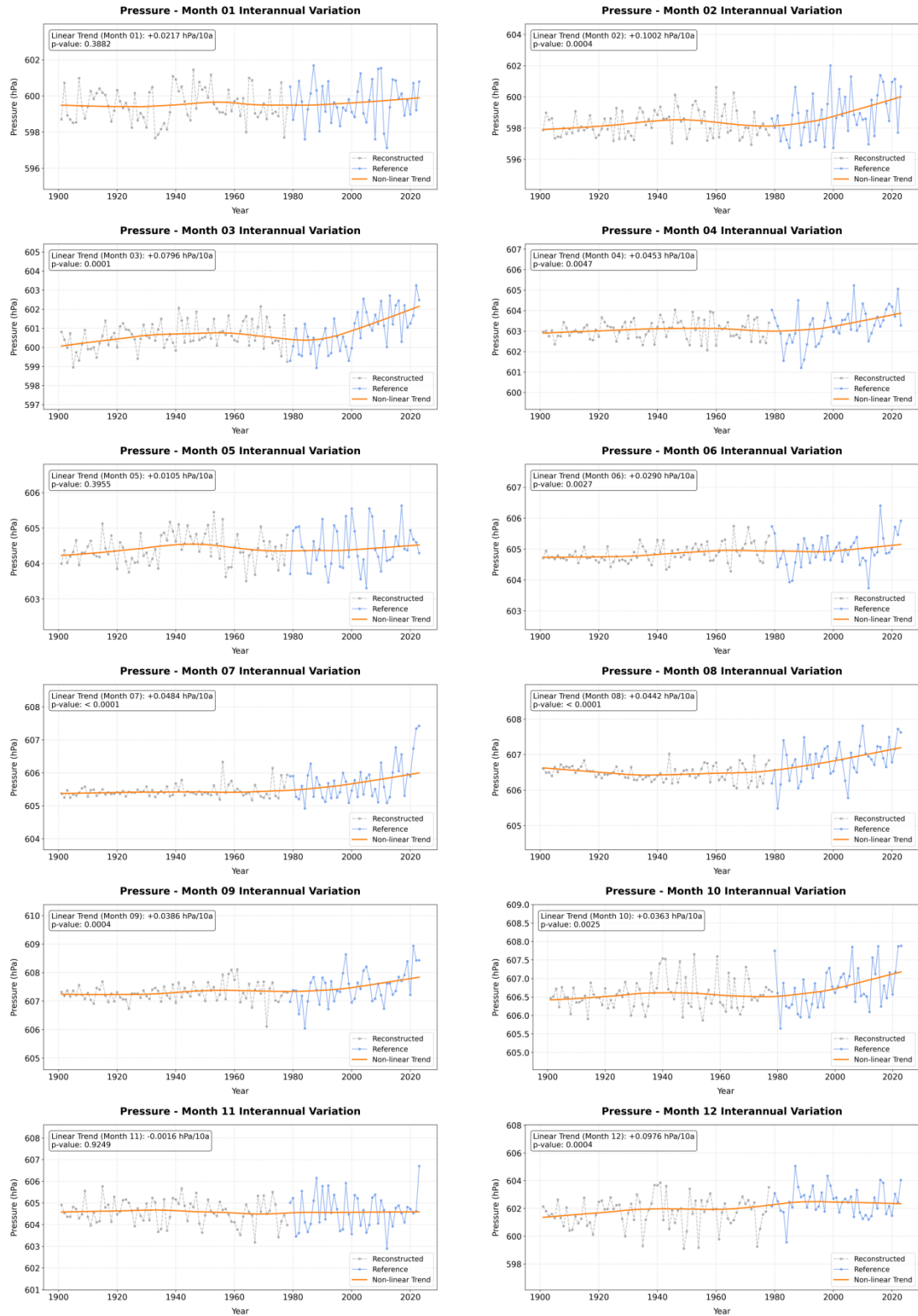


39

40 **Figure S5.** Monthly interannual variations of 2 m specific humidity over the Tibetan Plateau (1901–

41 2023). Grey dashed and solid blue lines denote the reconstructed (1901–1978) and reference (1979–2023)

42 data, respectively. The orange curve indicates the trend.

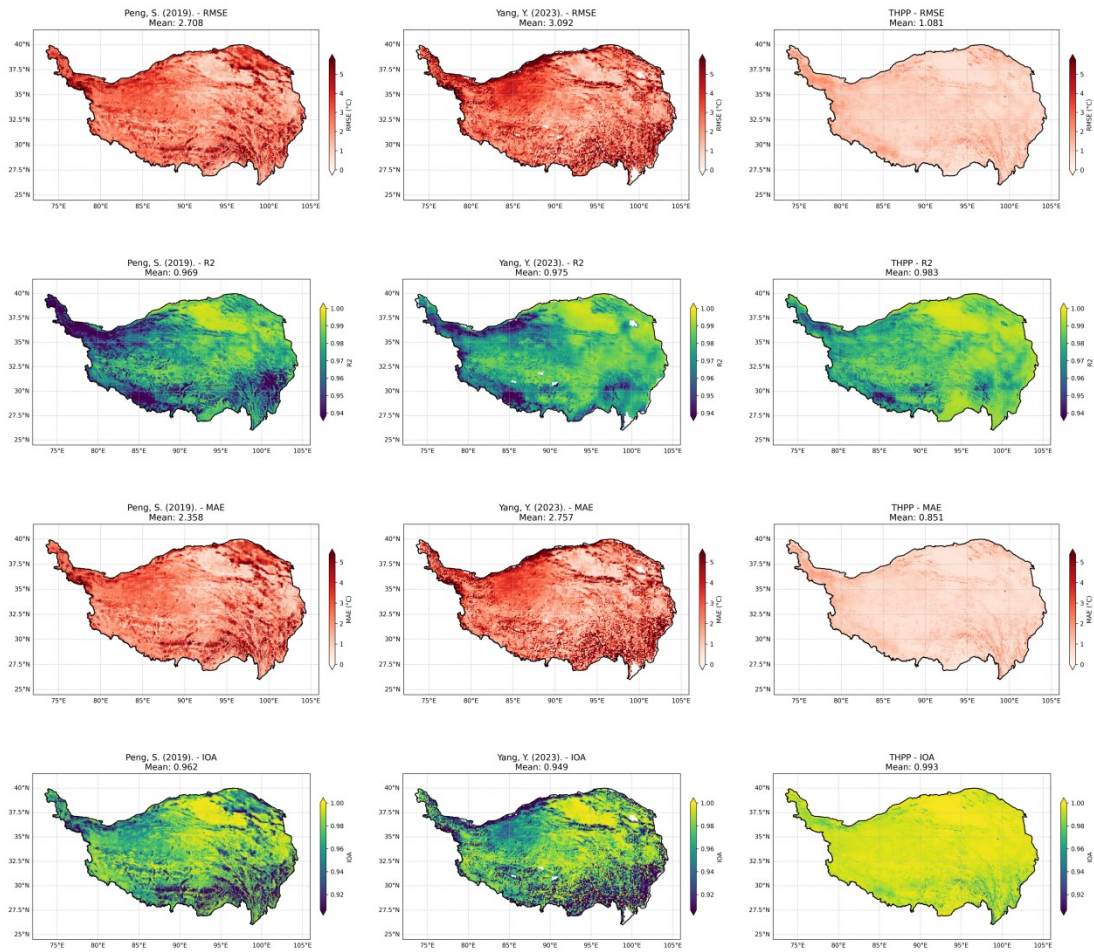


43

44 **Figure S6.** Monthly interannual variations of surface pressure over the Tibetan Plateau (1901–2023).

45 Grey dashed and solid blue lines denote the reconstructed (1901–1978) and reference (1979–2023) data,

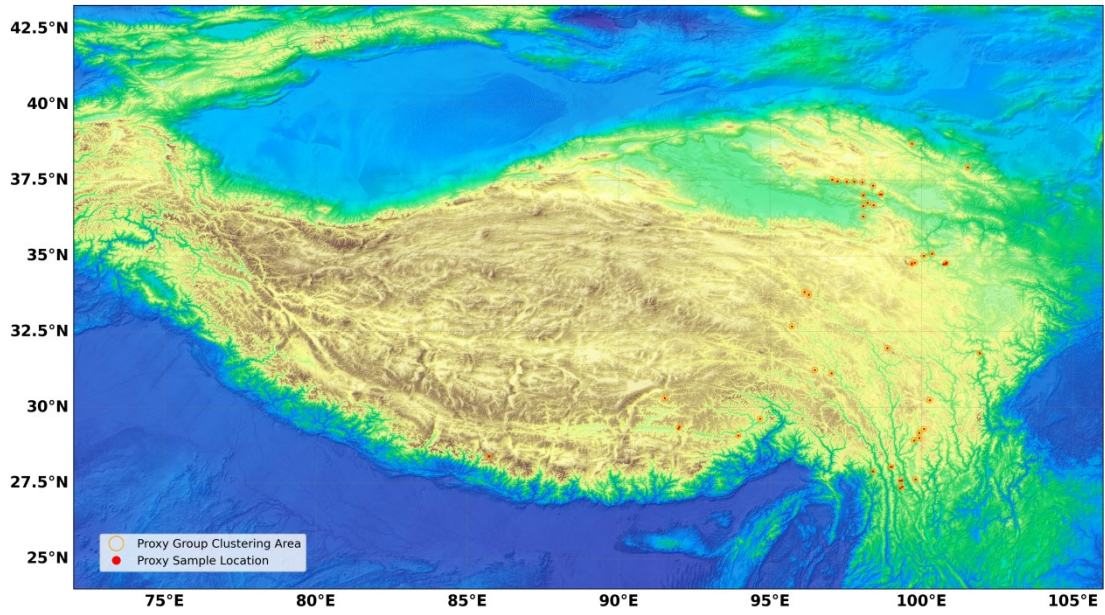
46 respectively. The orange curve indicates the trend.



47

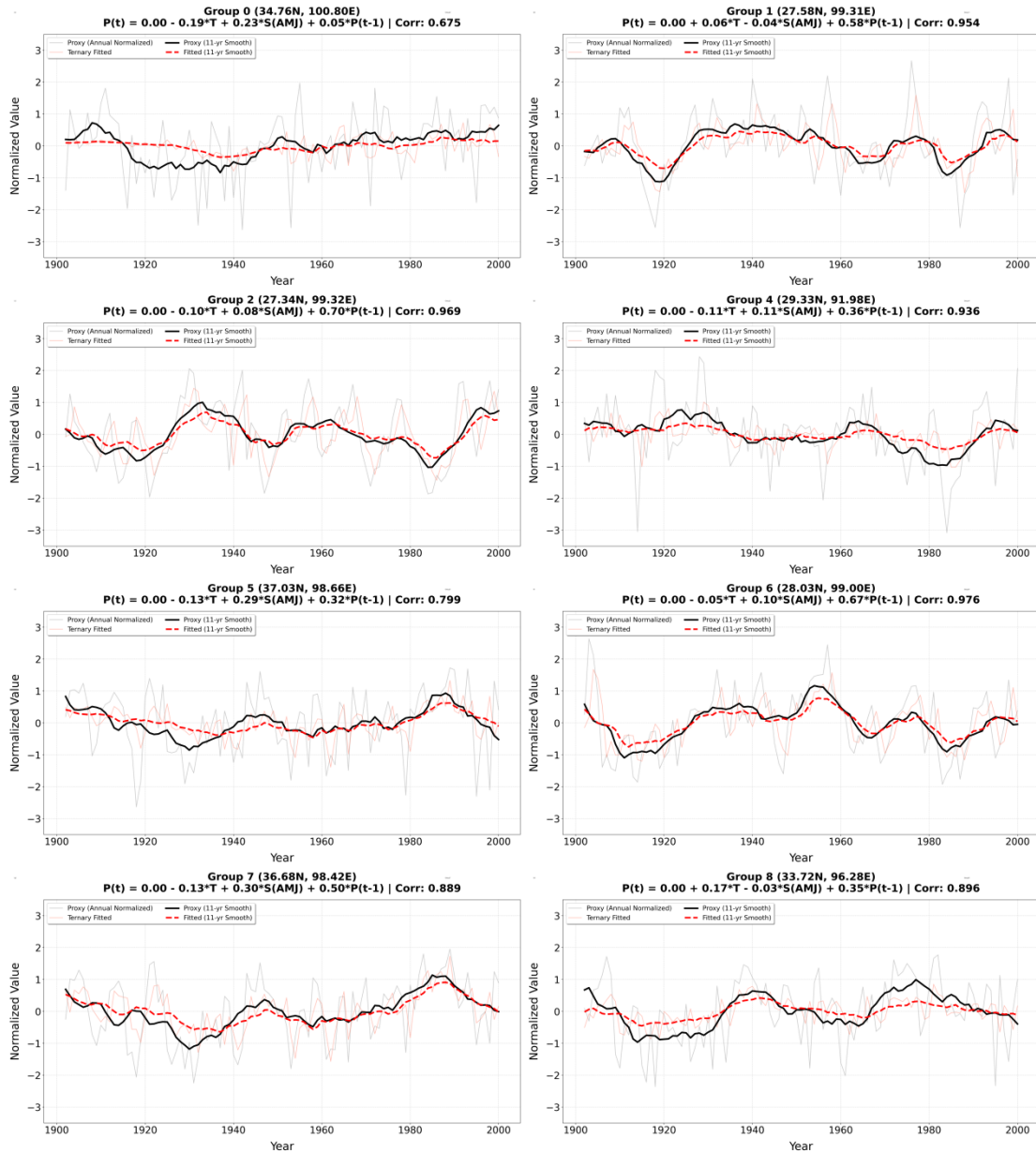
48 **Figure S7.** The panel compares the proposed THPP product against two representative datasets: a delta-
 49 downscaling-based product (Peng, S., 2019) and a GAN-based deep-learning product (Yang, Y., 2023),
 50 using TPMFD as the benchmark. Metrics include the coefficient of determination (R^2), Root Mean
 51 Square Error (RMSE), Mean Absolute Error (MAE), and Index of Agreement (IOA).

Spatial Proxy Sample Groups



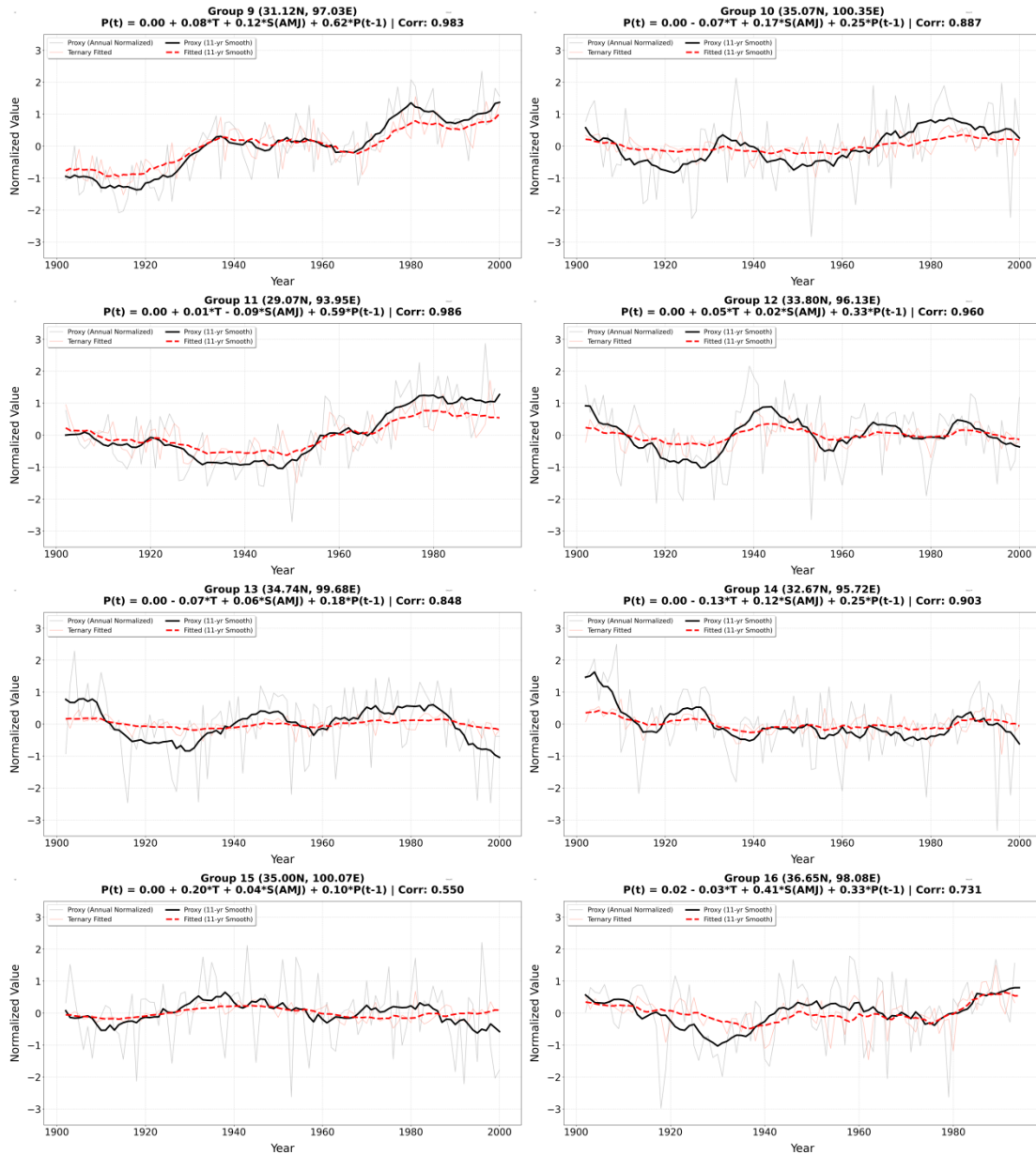
52

53 **Figure S8.** Geographical distribution of the 41 tree-ring proxy groups over the Tibetan Plateau used in
54 this study. Symbols represent the precise locations of chronologies (red dots), while circles (orange)
55 denote the spatial clustering areas defined for ternary regression fitting.



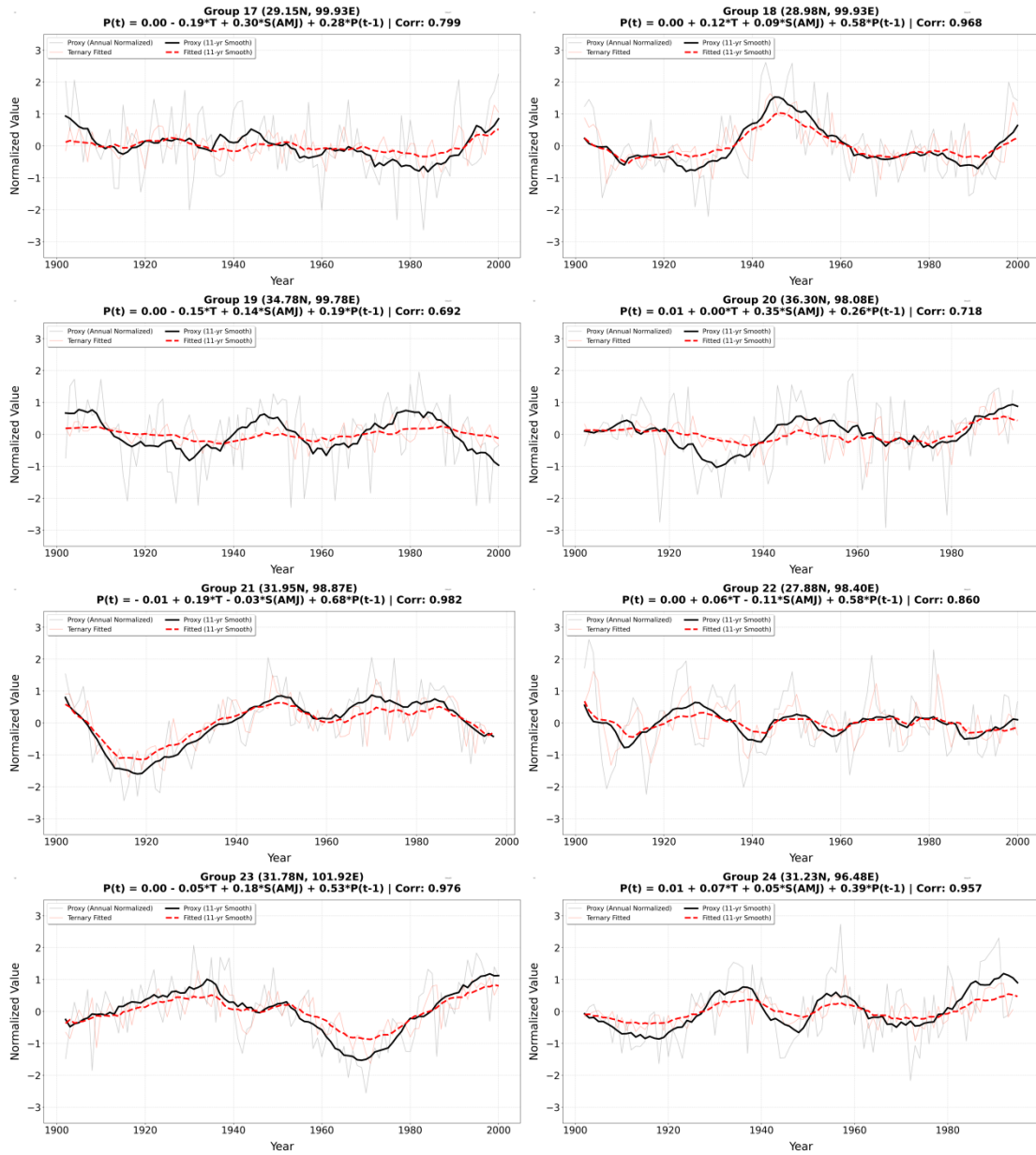
56

57 **Figure S9.** Temporal consistency between actual tree-ring proxy series and TPHH-based ternary fitted
 58 series for Groups 0–2 and 4–8 during 1901–2000. Each panel displays the annual normalized proxy
 59 values (light grey) and the 11-year moving average (black bold line), alongside the fitted series (light red
 60 line) and its 11-year smooth (red bold dashed line). The fitting equations, integrating JJA temperature
 61 (T), AMJ specific humidity (S), and lag -1 proxy memory (P(t-1)), are provided at the top of each subplot
 62 with their respective Pearson correlation coefficients (Corr). (Note: Group 3 is presented in Figure 12 of
 63 the main text).



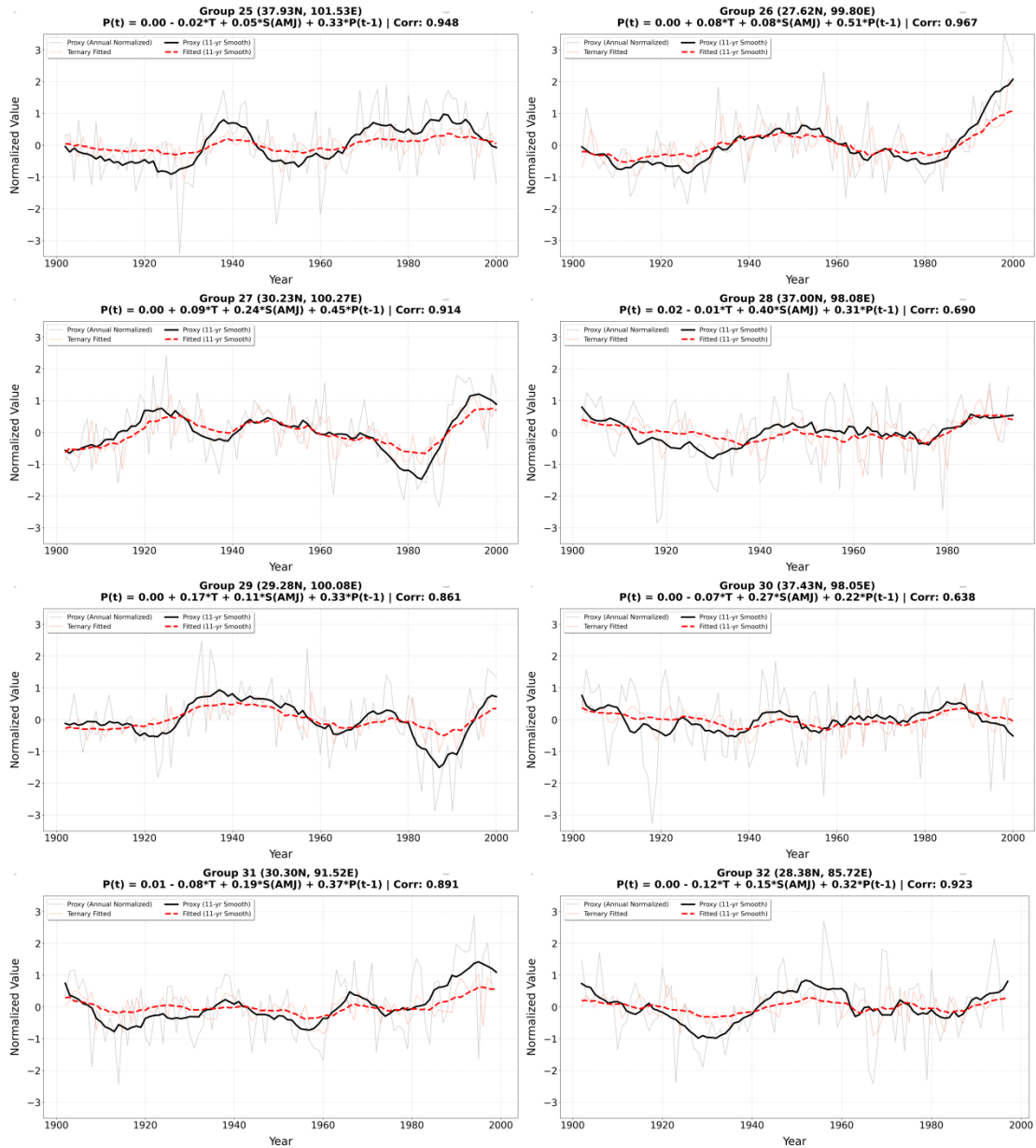
64

65 **Figure S10.** Temporal consistency between actual tree-ring proxy series and TPHH-based ternary fitted
 66 series for Groups 9-16 during 1901–2000. Each panel displays the annual normalized proxy values (light
 67 grey) and the 11-year moving average (black bold line), alongside the fitted series (light red line) and its
 68 11-year smooth (red bold dashed line). The fitting equations, integrating JJA temperature (T), AMJ
 69 specific humidity (S), and lag -1 proxy memory (P(t-1)), are provided at the top of each subplot with
 70 their respective Pearson correlation coefficients (Corr).



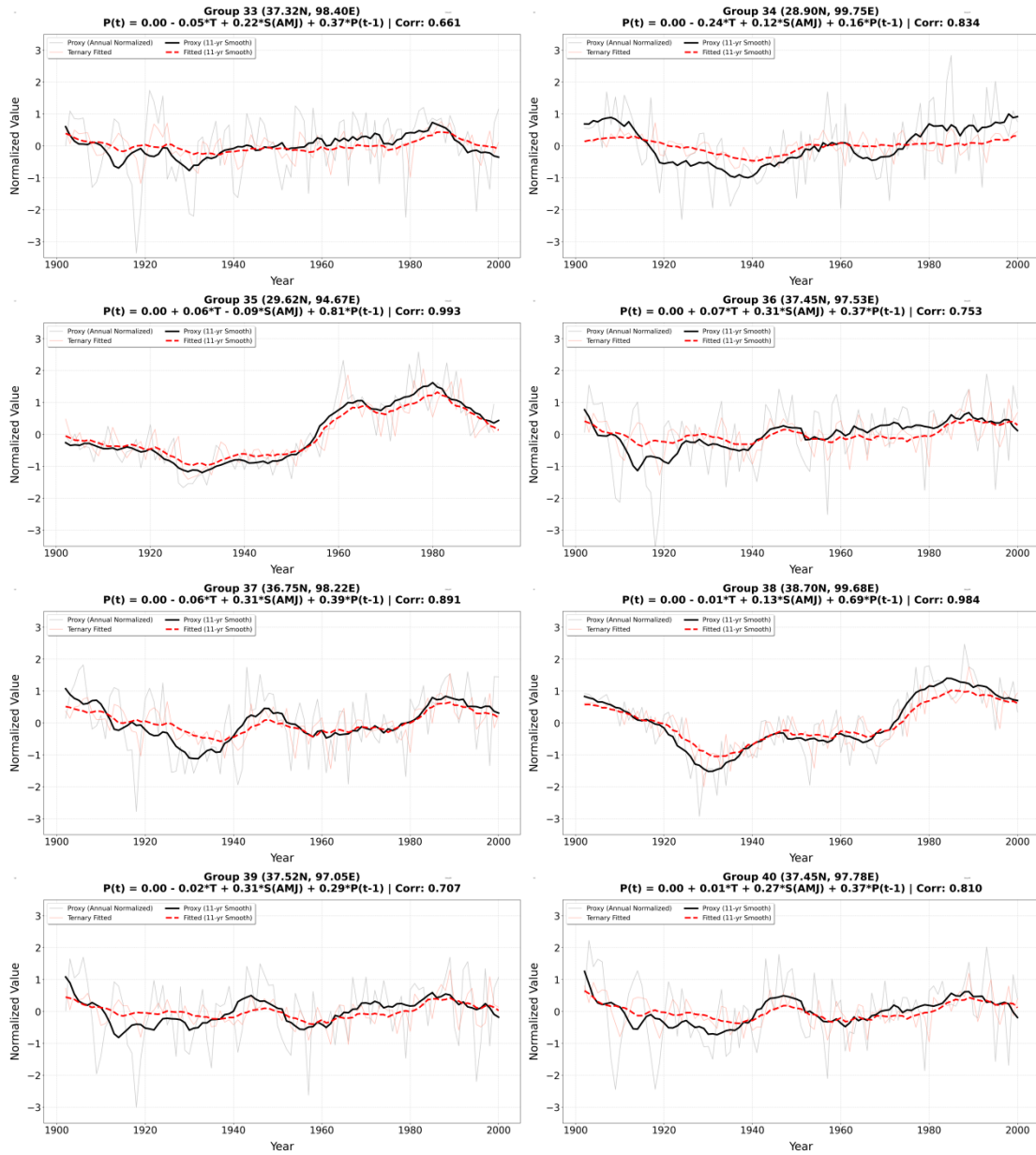
71

72 **Figure S11.** Temporal consistency between actual tree-ring proxy series and TPHH-based ternary fitted
 73 series for Groups 17-24 during 1901–2000. Each panel displays the annual normalized proxy values
 74 (light grey) and the 11-year moving average (black bold line), alongside the fitted series (light red line)
 75 and its 11-year smooth (red bold dashed line). The fitting equations, integrating JJA temperature (T),
 76 AMJ specific humidity (S), and lag -1 proxy memory (P(t-1)), are provided at the top of each subplot
 77 with their respective Pearson correlation coefficients (Corr).



78

79 **Figure S12.** Temporal consistency between actual tree-ring proxy series and TPHH-based ternary fitted
80 series for Groups 25-32 during 1901–2000. Each panel displays the annual normalized proxy values
81 (light grey) and the 11-year moving average (black bold line), alongside the fitted series (light red line)
82 and its 11-year smooth (red bold dashed line). The fitting equations, integrating JJA temperature (T),
83 AMJ specific humidity (S), and lag -1 proxy memory (P(t-1)), are provided at the top of each subplot
84 with their respective Pearson correlation coefficients (Corr).



85

86 **Figure S13.** Temporal consistency between actual tree-ring proxy series and TPHH-based ternary fitted
 87 series for Groups 33-40 during 1901–2000. Each panel displays the annual normalized proxy values
 88 (light grey) and the 11-year moving average (black bold line), alongside the fitted series (light red line)
 89 and its 11-year smooth (red bold dashed line). The fitting equations, integrating JJA temperature (T),
 90 AMJ specific humidity (S), and lag -1 proxy memory (P(t-1)), are provided at the top of each subplot
 91 with their respective Pearson correlation coefficients (Corr).